

FINAL REPORT

THE PEST PHENOMENON IN INTERMETALLICS

GPO PRICE \$ \_\_\_\_\_

CFSTI PRICE(S) \$ \_\_\_\_\_

Hard copy (HC) 2.00

Microfiche (MF) 1.50

ff 653 July 65

NASW - 1167

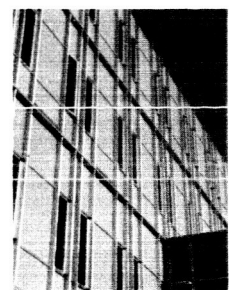
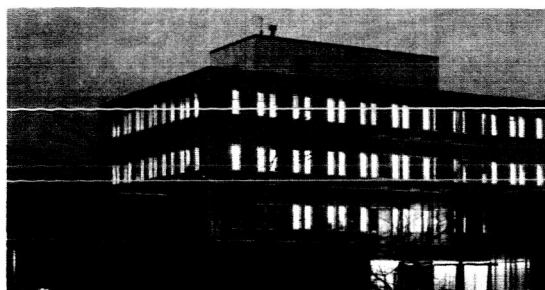
**N66 31769**

FACILITY FORM 602

(ACCESSION NUMBER)	(THRU)
<u>31</u>	<u>1</u>
(PAGES)	(CODE)
<u>CR-76427</u>	<u>17</u>
(NASA CR OR TMX OR AD NUMBER)	(CATEGORY)

May, 1966

**Arthur D. Little, Inc.**



This report is rendered upon the condition that it is not to be reproduced in whole or in part for advertising or other purposes without the special permission in writing of Arthur D. Little, Inc.

## INTRODUCTION

In prior work in this laboratory, <sup>(1)</sup> we established a number of characteristics of the pest phenomenon which led us to postulate that stress should have an important effect on oxidative failure in the pest range. In particular, we had shown previously <sup>(1)</sup> that stress-free single crystals of molybdenum disilicide do not pest. Under NASW-1167, we have been able to induce pest in single crystals by application of a bending stress. The results we have obtained to date indicate that the pest phenomenon is related to the phenomenon of static fatigue or delayed failure in brittle materials as studied by Charles and Hillig. <sup>(2)</sup>

## EXPERIMENTAL

### Materials Preparation

Single crystal rods of molybdenum disilicide were prepared by zone melting of sintered compacts. The starting material was 200 mesh  $\text{MoSi}_2$  powder of 99.5% purity purchased from Sylvania. This was mixed with duPont semi-conductor grade silicon in sufficient amount to compensate for evaporative losses during synthesis. The powder is sintered to about 70% theoretical density in a boron nitride mold. The sintered compact, about 8 inches long and 1/2 inch in diameter, is zone melted in a flowing argon atmosphere by passing a slowly moving induction coil up along its length. The molten zone moves at about 1 inch/hr. The fabricated material contains impurities in the ppm range of Al, Cr, Mn, Fe, and Cu as determined spectroscopically. Typical oxygen analyses lie in the 10-100 ppm range. The samples are single crystal, single phase  $\text{MoSi}_2$  as shown by X-ray and metallography.

Bar specimens 1/2 -- 1 inch x 1/8 inch x 1/8 inch were cut from the zone melted rods for the bend tests described below. Considerable difficulty has been experienced in obtaining bars free from gross macro-cracks, suitable for the mechanical tests. The cracks are probably due to the stresses set up by the zone-melting and rapid cooling of a material which is anisotropic in thermal expansion.

### Static Bend Tests

The rectangular bar specimens discussed above were tested in bending under four point load. The apparatus consists of a 304 stainless steel jig with aluminum oxide (Lucalox) knife edges. There is a distance of 3/8 inch between the lower knife edges and 1/8 inch between the upper ones. The four point load should provide a constant bend moment across the inner span; the maximum outer fiber stress was calculated from the usual formula for stressed beams. For the tests in air the bend fixture was surrounded by a wire-wound alumina core resistance furnace that provides temperatures up to 650°. Dead weight loading was used. Base level data were obtained in vacuum with the same jig mounted in the Instron and enclosed in a tungsten resistance furnace.

Delayed failure tests were run at 500°C in air on single crystal bars of molybdenum disilicide. The results are tabulated in the first two columns of Table I, taken from our Progress Report 3.

<u>TABLE I</u>		
<u>Applied Stress (S)</u>	<u>Failure Time (<math>\tau</math>)</u>	<u>S/S<sub>N</sub></u>
32,600	0.1 hr.	0.615
26,000	12	0.49
20,900	168	0.39
20,100	1040	0.38

In every case, when failure did occur the fracture surfaces were covered with the powdery yellow oxide ( $\text{MoO}_3 + \text{SiO}_2$ ) which is invariably associated with "pest".

The Charles-Hillig theory for static fatigue in brittle materials relates the ratio of applied stress to inert atmosphere strength,  $S/S_N$ , to the logarithm of the delayed failure time,  $\log \tau$ . In order to use the theory to analyze the delayed failure data on single crystal molybdenum disilicide listed in Table I, it is necessary to have a value for the base level strength,  $S_N$ .

Base level data were obtained at 500°C in vacuum. The statistical nature of fracture strength in brittle materials is well recognized. By the Griffith criterion, fracture under given conditions of stress

depends on flaw geometry. Since the flaw distribution can be expected to vary considerably from one finite sized sample to another, measured values of strength ( $S_N$ ) as well as delayed failure times under load will be statistically grouped about some most probable value. In order to assess the variation in  $S_N$  for the single crystal samples that we have available, the bend strength of nine single crystal bars of molybdenum disilicide was measured in vacuum at 510°C. The same jig used in the delayed failure tests was used in conjunction with the Instron. The system was evacuated to about  $2 \times 10^{-5}$  torr. The cross-head speed was 0.1 cm/min. Results are summarized in Table II. The bend strength varies by a factor 35 between the strongest and weakest samples tested.

It is clear that none of the delayed failure tests listed in Table I was made on a sample with  $S_N$  as low as 19,100 psi. It also seems very unlikely that many samples were produced with  $S_N$  as high as 147,500 psi. If we assign a weight of 1 to the highest measured bend strength, and a weight of 2 to the three next lowest points, we obtain an average base level strength of  $53,000 \pm 29,000$  psi. This value of  $S_N$  was used to analyze the data in Table I.

In Figure 1, the ratio of applied stress to room temperature strength,  $S/S_N$ , is plotted against the logarithm of the delayed failure time,  $\log \tau$  for the data of Table I. A characteristic static fatigue curve is obtained. The fatigue limit  $S/S_N \approx 0.35$  and the slope of the straight line portion of the curve (indicated with a dotted line in the Figure) are related to basic parameters of the Charles-Hillig theory for static fatigue in brittle materials [R. J. Charles, Applied Phys. 29, 1549, p. 1554 (1958)]. We calculate an activation volume for pest failure of 2.4 cc. and an interfacial free energy between  $\text{MoSi}_2$  and the pest oxide of 1800 ergs/cm<sup>2</sup>.

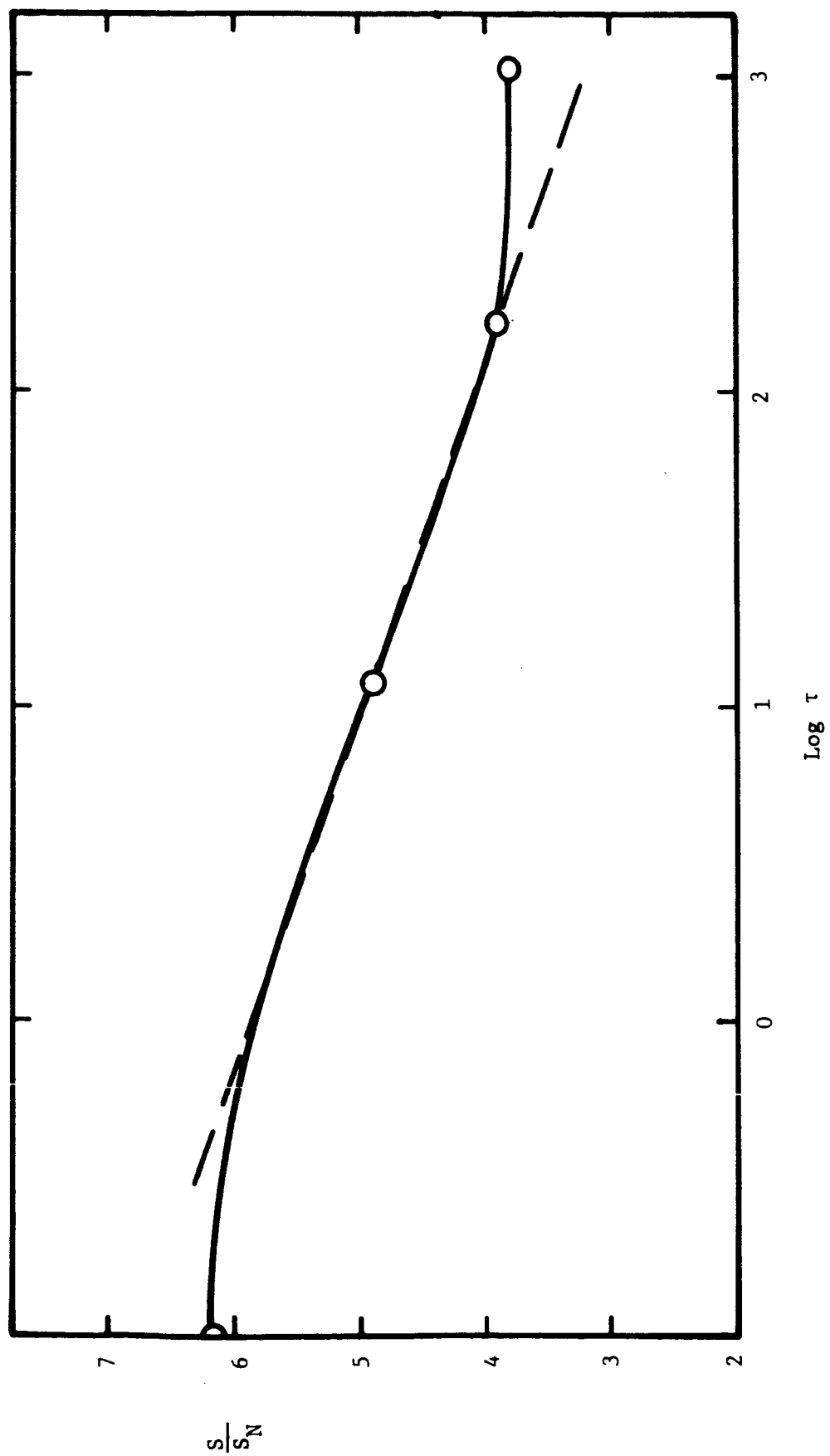


FIGURE 1

TABLE II

BASE LEVEL STRENGTH OF SINGLE CRYSTAL MoSi<sub>2</sub> IN 4-POINT BENDING

T = 510°C

p =  $2 \times 10^{-5}$  torr

Cross-head speed = 0.1 cm/min

<u>Sample No.</u>	<u><math>\sigma</math> (psi)</u>
1033-2-1	147,500
1031	58,800
1038-1A-48	29,000
1034-A-39	24,000
1040	19,100
1038-1A-47	15,200
1041	8,800
1034	4,250
1039	4,230

Our derived value of 2.4 cc compares well to the value of 1 cc obtained by Charles and Hillig for steam corrosion of soda-lime glasses. Our derived surface energy of 1800 ergs/cm<sup>2</sup> compares well with the Charles-Hillig value of 500 ergs/cm<sup>2</sup> for the glasses. The significance of the results and the probable limits of error are taken up in the discussion section below.

Over the last three months further delayed failure experiments have been done at 500° and 600°C in air.

A single crystal bar (#1033-2-1) was dead weight loaded at 30,000 psi and held at 500°C in air for 2040 hours without fracturing. At the end of that time, the bar was mounted in the same jig in the Instron, and its tensile strength was measured at 500°C in vacuum. With a cross-head speed of 0.1 cm/min, the tensile strength of 147,500 psi listed above was measured. Thus, for this specimen  $S/S_N \approx \frac{30,000}{147,500} = 0.2$ , and the failure to observe a delayed fracture in more than 2000 hours is consistent with the previous results

At 600°C in air under a dead weight load of 15,600 psi, a single crystal bar (#1034-1A-40) showed a delayed failure time of 250 hours. In the absence of precise base level data (i.e.  $S_N$  values) it is difficult to compare this result with those obtained at 500°C. The existence of a delayed failure effect however has been demonstrated. Furthermore, since the fracture surfaces were covered with the yellow "pest" oxide, the delayed failure may be considered a stress induced pest type failure in a single crystal.

Under an applied bend stress of 11,000 psi, no delayed failure was found in 2850 hours at 600°C for a single crystal bar (#1038-1A-48). Its measured bend strength at the end of this time was 29,000 psi. Although the surface of the sample was covered with a uniform deep blue adherent oxide film, there was no evidence anywhere for the yellow "pest" oxide. The results at 600°C suggest that at a given  $S/S_N$  value, the delayed failure time will be longer at 600°C than 500°C. This would be consistent with the fact that pest disintegration in polycrystals and sintered samples is generally slower at 600 than at 500°C. The failure to observe a delayed fracture in this experiment in 2850 hours with

$S/S_N \approx 11,000/29,000 = 0.38$  also indicates that the delayed failure effects reported above are not due to creep but are true environmental effects on brittle fracture. In Table I a delayed failure time of 1040 hours was observed at 500°C with  $S/S_N = 0.38$ . If this were due to creep, then at 600°C failure would have occurred in a shorter time. Experimentally, no failure was seen in more than twice the time.

## Thermal Stresses in Polycrystalline MoSi<sub>2</sub>

In order that the proposed mechanism of pesting be applicable to polycrystalline MoSi<sub>2</sub>, some source of an internal stress must exist since it has been shown that polycrystals pest in the absence of an external stress. One source of internal stress is that due to anisotropic elastic modulus and thermal expansion along different crystallographic directions. When polycrystalline material is cooled from high temperatures, the individual grains are able to relieve stresses built up by differential contraction between adjacent grains, until a temperature is reached where relaxation of the stress is no longer possible. The order of magnitude of these thermal stresses will largely be a function of the difference in the expansion coefficient along different crystallographic directions and the temperature range over which relaxation could not take place. Differential expansions of the order of 10-20% are sufficient to develop stresses which may be as large as or greater than the fracture stress of the material.

Thermal expansion in the "a" and "c" directions of MoSi<sub>2</sub> was determined by measuring changes in the "d" spacing of selected reflections with increasing temperature by X-ray diffraction techniques. By observing the lattice spacing at several temperatures the thermal expansion coefficient along different crystallographic directions can be determined.

The "d" spacing is determined for a particular lattice plane in the crystal by the Bragg law  $d = \frac{n \lambda}{2 \sin \theta}$  - where  $\theta$  is the angle between the diffracted beam and the diffracting plane. For MoSi<sub>2</sub> which has a tetragonal crystal structure

$$\frac{1}{d^2} = \frac{h^2 + k^2}{a^2} + \frac{l^2}{c^2}$$

"a" and "c" are the lattice parameters and (h, k, l) are the Miller indices for the reflecting plane. For lattice planes in which changes in the "d" spacing are due to expansion in only one crystallographic direction [(h, 0, 0) or (h, k, 0) for the "a" direction and (0, 0, l) for the "c" direction] the change in "d" between two temperatures

$T_1$  and  $T_2$  is given by

$$\frac{\Delta d}{d} = \frac{\sin \theta_{T_1}}{\sin \theta_{T_2}} - 1$$

An MRC high temperature X-ray furnace was fitted to a standard Norelco diffractometer. Fe  $K_\alpha$  radiation was used and the diffracted signal was detected with a single chamber Geiger counter. The signal was fed to a rate meter and recorded on strip charts. A platinum strip heater in the furnace was coated with a layer of -325 mesh  $\text{MoSi}_2$  powder, obtained by grinding a single crystal. Temperatures were measured by a Pt- Pt 13% Rh thermocouple located on the specimen: A helium atmosphere was maintained in the furnace during runs. Diffraction peaks were scanned at a rate of 1/8 degree ( $2\theta$ ) per min. and a chart speed of 0.1 degree ( $2\theta$ )/cm. Diffraction patterns were obtained at room temperature and at 200° intervals up to 800°C.

Figure 2 is a plot of  $\left[ \frac{\sin \theta_{T_1}}{\sin \theta_{T_2}} - 1 \right]$

versus temperature for the reflection (110) and (002). The former gives  $\frac{\Delta d}{d}$  in the "a" direction and the latter the change in "d" spacing in the "c" direction. It is obvious that very little anisotropy of the expansion coefficient is observed. Differences in  $\frac{\Delta d}{d}$  in the two directions are within the experimental error. The data agree with those of Bartlett which were carried out on polycrystalline coatings.

It is difficult to rationalize the lack of crystallographic anisotropy of the thermal expansion in a material such as  $\text{MoSi}_2$ . The crystal structure has a high c/a ratio and a layer like structure which would lead one to expect large differences in properties along the two crystallographic directions. However, a differential expansion of 10% (within experimental error) would be sufficient to produce stress of the order of 20,000 psi in  $\text{MoSi}_2$  and these stresses would be a significant fraction of the fracture stress.

The presence of an internal stress appears to be essential to the proposed mechanism, and in view of the experimental difficulties of

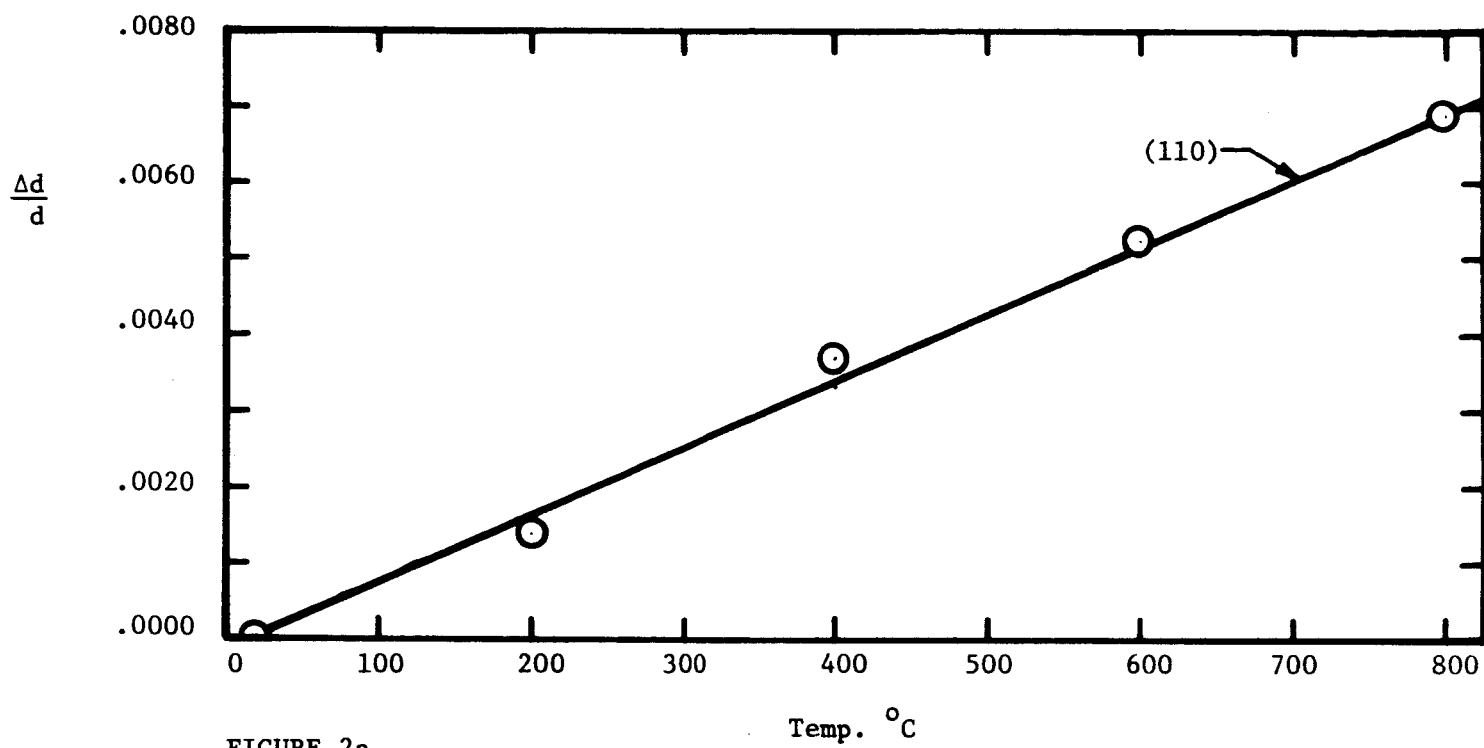


FIGURE 2a

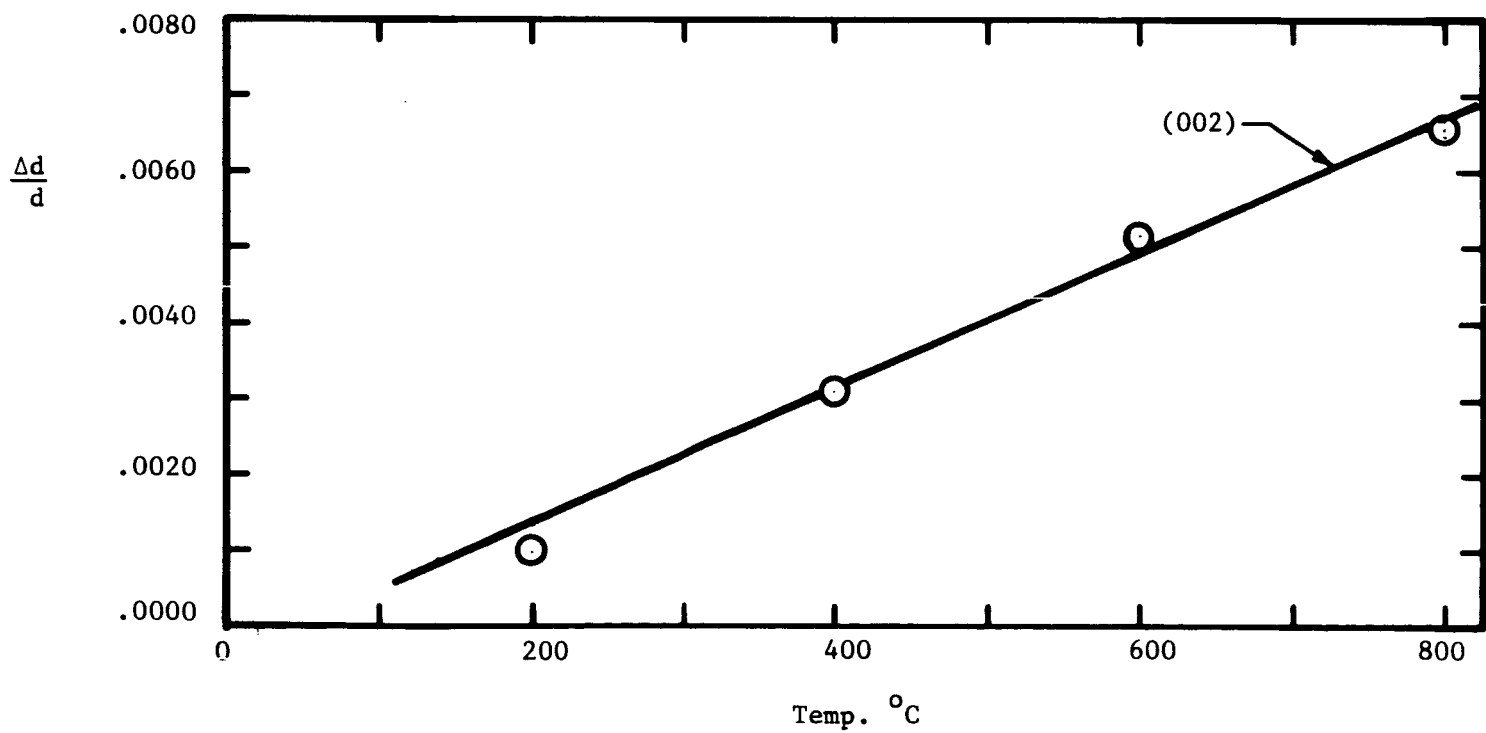


FIGURE 2b

measuring small shifts in "d" spacing in the X-ray method, we believe that further efforts should be made to investigate the possibility of thermal expansion anisotropy. A quartz dilatometer is available in the laboratory and we plan to measure directly the thermal expansion of an oriented single crystal.

### SIMULTANEOUS WEIGHT CHANGE AND OXYGEN CONSUMPTION MEASUREMENTS

The Charles-Hillig development relates the rate of oxidation in the neighborhood of a crack tip to the velocity of crack propagation. One of the important parameters required in analysis of the data is the activation energy for delayed failure. This should be equal to the activation energy for oxidation. It is not possible to obtain a meaningful activation energy from the customary weight change curve alone, because the volatility of molybdenum trioxide varies considerably over the test range; it is negligible at 300°C, the lower temperature limit, but very appreciable at 600°C, the approximate upper temperature limit. In order to better define the chemical oxidation reaction, we are measuring total oxygen consumption and net weight change simultaneously on the same samples. This data can be analyzed to establish the rates of formation of both solid and volatile oxides.

A simple apparatus was constructed in which weight changes are measured by the extension of a quartz helical spring and oxygen consumption is followed with a differential manometer. A schematic diagram is shown in Figure 3. Samples of  $\text{MoSi}_2$  nuggets weighing about 0.2 g are contained in an open platinum bucket which is suspended from the spring. One arm of the manometer is connected to the reaction chamber; the other arm is connected to a blank chamber at the same temperature and initial pressure. The reaction and control chambers are heated by a surrounding tube furnace. The quartz spring used presently has a sensitivity of  $10^{-5}$  g. Extension of the spring is measured by sighting a cathetometer on a reference mark. The manometric fluid is DOW 704 which has a sensitivity about ten times that of mercury. The volume of the reaction chamber was determined by filling both chambers with oxygen to a pressure of one atmosphere, and measuring the pressure change when the gas in the reaction chamber was allowed to expand into a connecting evacuated bulb of known volume.

Simultaneous weight change and oxygen consumption measurements obtained on  $\text{MoSi}_2$  in oxygen at one atmosphere at temperatures of 500, 550, 600, and 650°C are plotted in Figure 4. The oxygen pickup must always be greater than or equal to the net weight change as observed. If no

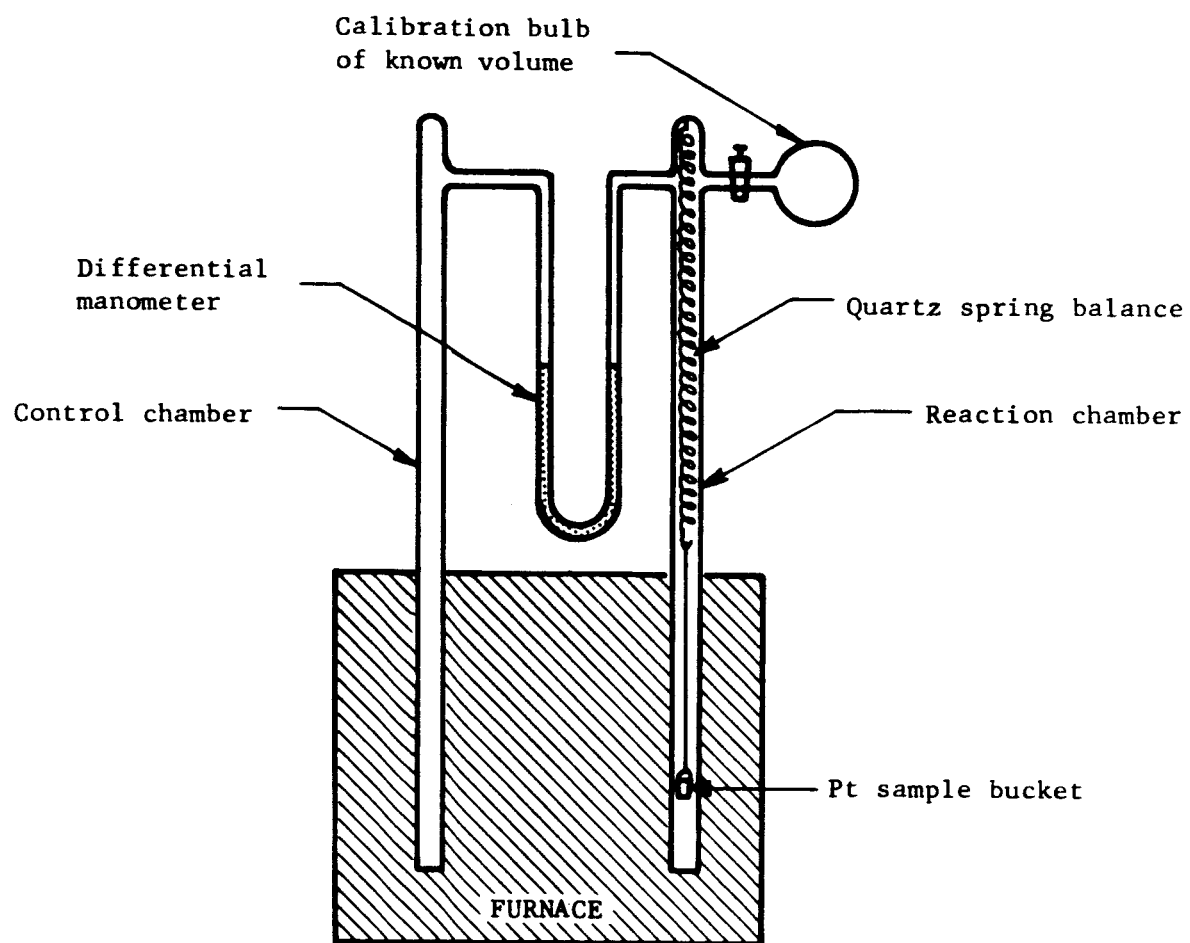


FIGURE 3

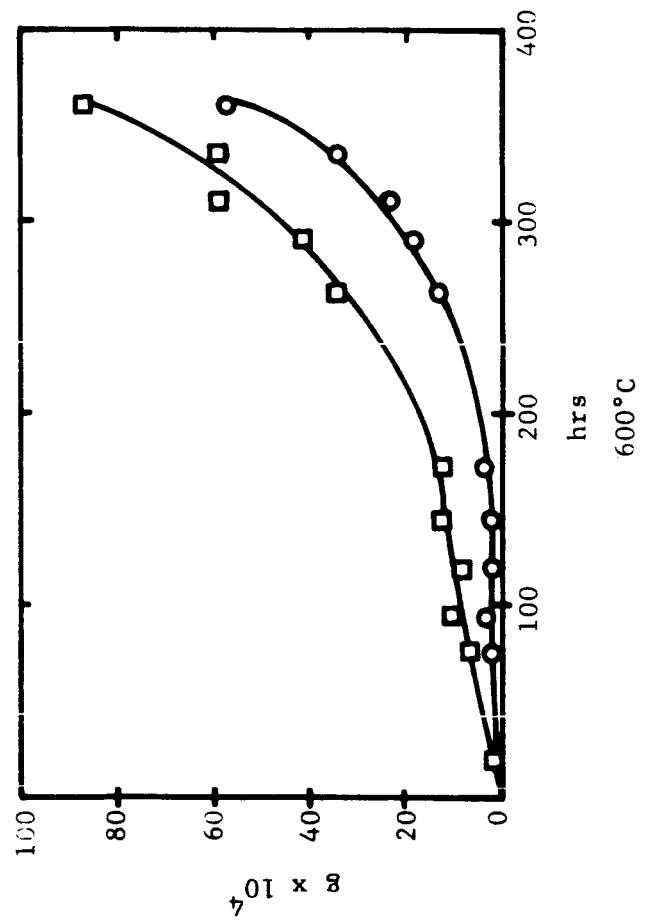
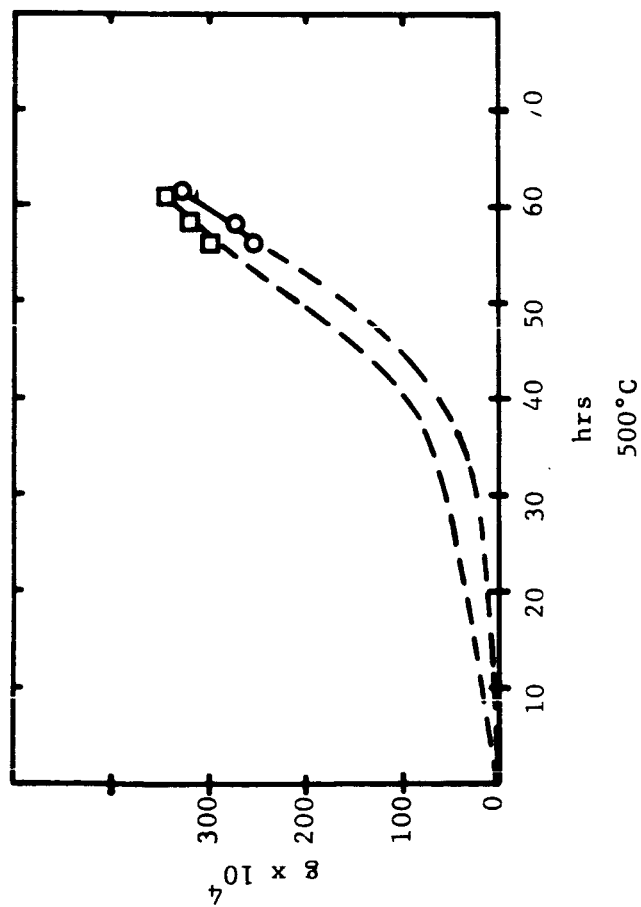
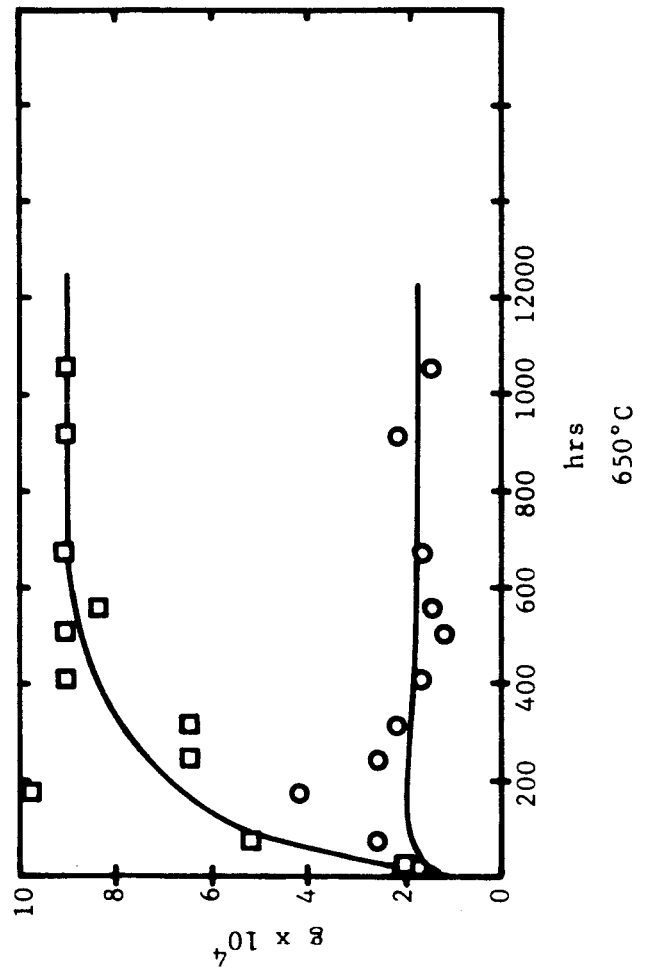
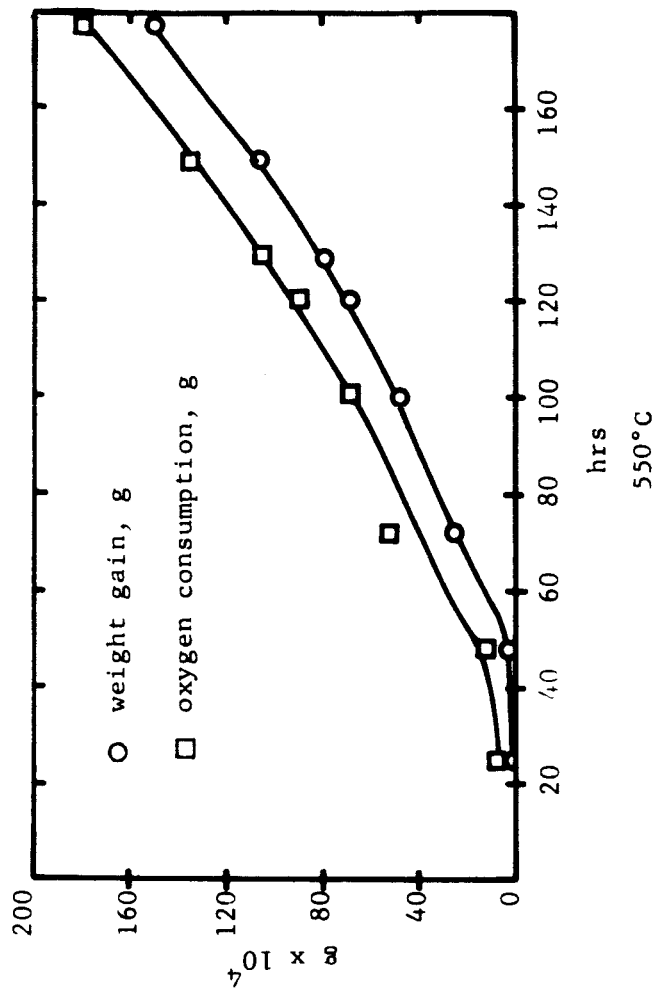


FIGURE 4

molybdenum trioxide were to vaporize, the weight change would be identical with the oxygen pickup. Any loss of molybdenum, as the trioxide, would lead to a decrease in sample weight without affecting the total oxygen pickup. If we define:

$\Delta w$  = net weight change, g

$\Delta m$  = total oxygen pickup, g

$x_g$  = amount of oxygen tied up in volatile  $\text{MoO}_3$  (g)

$x_s$  = amount of oxygen bound to the surface as solid oxides

we may write:

$$\Delta w = x_s - \frac{[\text{Mo}]}{3[\text{O}]} x_g \quad (1)$$

$$\Delta m = x_s + x_g \quad (2)$$

where the symbols in brackets are molecular weights. From the data in Figure 4, equations (1) and (2) may be solved for  $x_s$  and  $x_g$ , respectively, the total oxygen consumed in the formation of solid and volatile oxides. Final results for the data in Figure 4 are given in Table III. The  $x_s/x_g$  ratios given in the last column clearly demonstrate the increased importance of molybdenum trioxide vaporization as the temperature increases. At 500°C more than 99% of the oxygen consumed remains on the silicide surface; at 650°C almost 30% of the oxygen consumed goes into the formation of volatile oxides. It is interesting to note that pest fracture was not observed at 650°C, consistent with the absence of a region of accelerating rate. Typical pest behavior was seen at lower temperatures.

Berkowitz, Blackburn, and Felten<sup>(1)</sup> showed that at 500°C the time to rapid pest disintegration is a highly sensitive function of oxygen partial pressure at a total pressure of one atmosphere. It might be expected that at this temperature solid  $\text{MoO}_3$  (s) should be present and hence, the rate of vaporization of molybdenum trioxide should be constant; i.e., the rate of build-up of solid oxide would have the same functional form as the net rate of weight change. If, as seems reasonable, the presence of solid  $\text{MoO}_3$  in the pest range contributes to pest

TABLE III  
RELATIVE AMOUNTS OF SOLID AND VOLATILE OXIDES  
FORMED DURING PESTING IN OXYGEN (1 atm)

<u>T, °C</u>	<u>Exposure time, hrs</u>	<u>Initial sample weight, g</u>	<u>x<sub>s</sub>, g</u>	<u>x<sub>g</sub>, g</u>	<u>x<sub>s</sub>/x<sub>g</sub></u>
500	61	0.1703	0.0332	0.0001	332
550	177	0.1711	0.0170	0.0010	17
600	361	0.1639	0.00769	0.00101	7.6
650	1063	0.2162	0.00066	0.00025	2.6

x<sub>s</sub> = amount of oxygen in solid oxides.

x<sub>g</sub> = amount of oxygen in volatile oxides.

failure, then pest kinetics should be sensitive to the relative rates of formation of solid and volatile oxide. By varying total pressure at given oxygen partial pressures and temperatures, it should be possible to alter the rate of removal of molybdenum trioxide by vaporization. We have therefore started to obtain net weight change curves as a function of absolute oxygen pressure.

At 500°C the curve in Figure 5 at an oxygen total pressure of 0.1 atm may be compared with the curve in Figure 4 at an oxygen total pressure of 1 atmosphere. In neither case is there any significant loss of molybdenum trioxide by vaporization. The absolute level of the weight gain or oxygen consumption is of little importance, since it depends on sample surface area. However, the point of inflection, or point of transition between the initial slow oxidation rate and the final accelerating rate, is noteworthy. The region of accelerating rate sets in after about 35 hours at 1 atm oxygen, but does not set in for 300 hours at 0.1 atm oxygen.

At 550°C the curve in Figure 6 for an oxygen partial pressure of 0.1 atm, total pressure 1 atm may be compared with the curve in Figure 4 for an oxygen total pressure of 1 atm. In both cases there is a very small difference between the total oxygen consumed and the net weight change. The point of inflection is about 700 hours at the lower partial pressure and about 50 hours in the pure oxygen.

At 600°C the curve of Figure 7 taken at a total oxygen pressure of 0.1 atm differs considerably from the curve of Figure 4 taken at a total oxygen pressure of 1 atm. At the lower pressure there is no point of inflection up to 300 hours; at the higher pressure a region of accelerating rate appeared at about 200 hours. Although the data in Figure 7 are very erratic, there seems to be more rapid loss of volatile oxide at the lower pressure than at the higher. The  $x_s/x_g$  ratio is 2.8 at 0.1 atm and 7.6 at 1 atm.

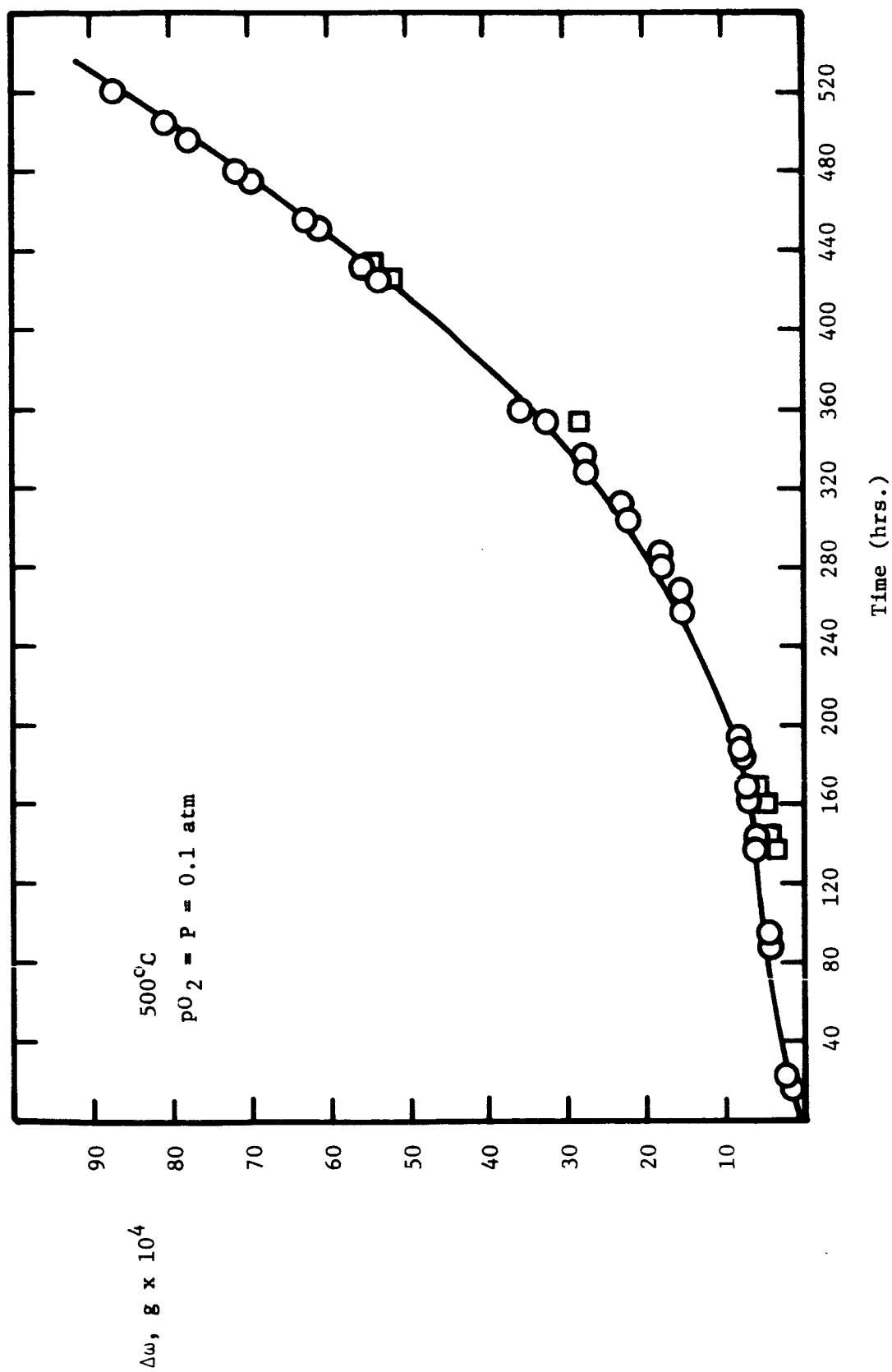


FIGURE 5

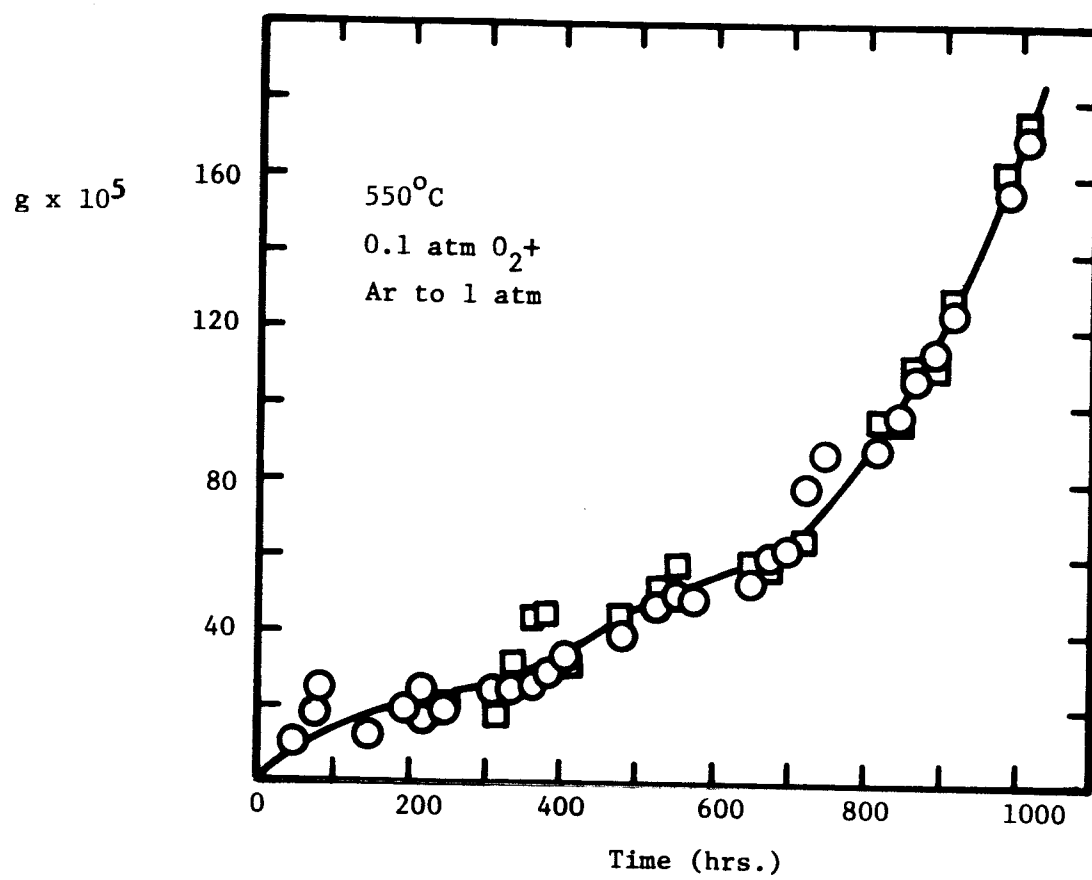


FIGURE 6

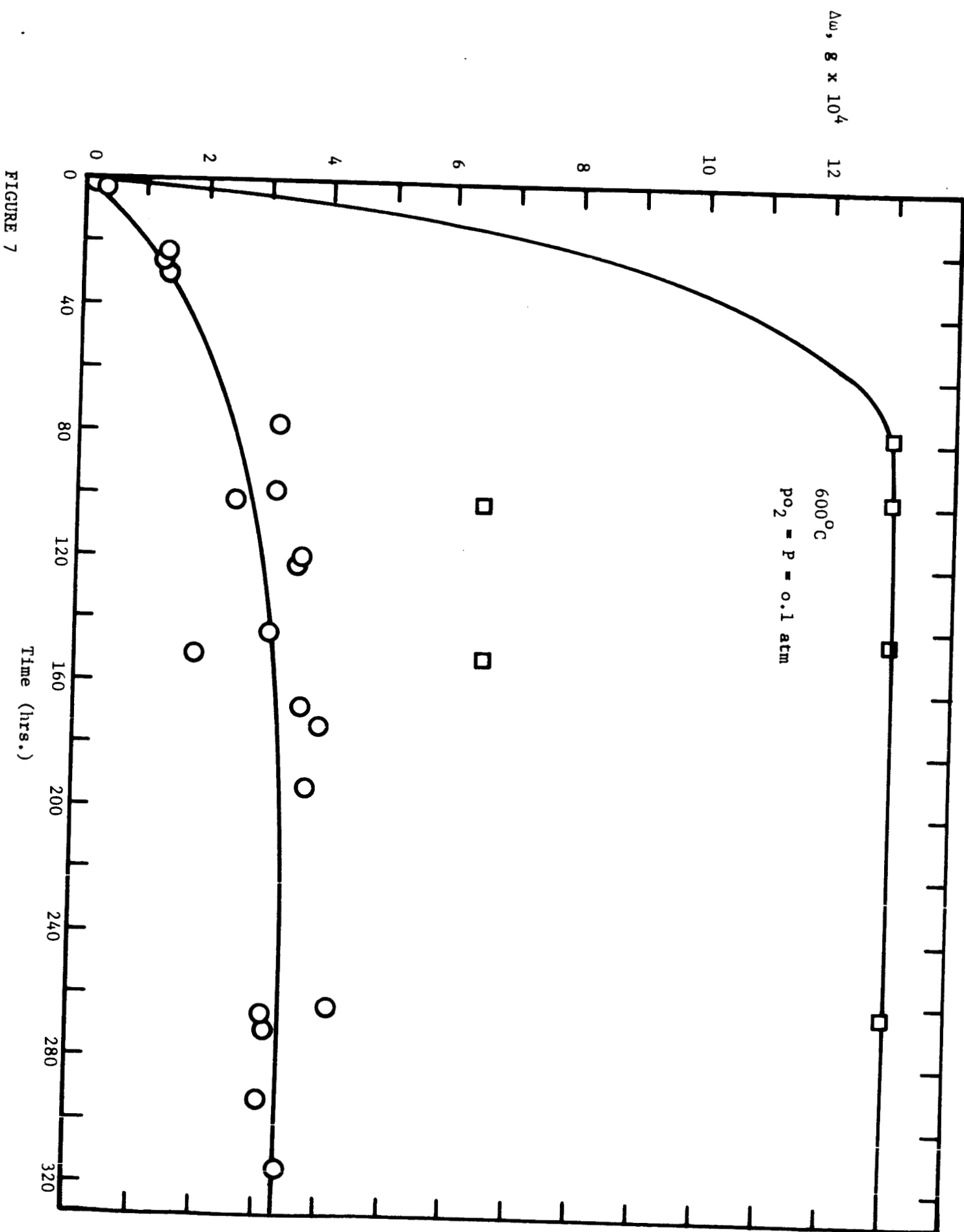


FIGURE 7

## DISCUSSION

The results obtained to date on oxidation of single crystals of  $\text{MoSi}_2$  in the pest range seem to conform to the theory developed by Charles and Hillig,<sup>(2)</sup> relating the rate of oxidation in the neighborhood of a crack tip to the velocity of crack propagation. In the absence of a chemical oxidation reaction, the Griffith flaw theory establishes the conditions for growth of a pre-existing crack of a given length. Charles and Hillig point out that chemical reaction can influence flaw growth and lead to delayed failure or static fatigue. It seems clear that oxidation in the neighborhood of a flaw must alter the flaw geometry. However, a delayed failure will result only if the geometry of the flaw is altered in such a way as to produce an increase in stress concentration. That is, the tip of the flaw must advance more rapidly than the sides.

If the activation energy for chemical oxidation is stress sensitive, we denote it by  $E^*$  (6) and may expand it in a Taylor's series as follows:

$$E^* (6) = E^* (0) + 6 \left. \frac{\partial E^*}{\partial \sigma} \right|_{\sigma = 0} + \dots$$

The first term is independent of stress; the second term has the dimensions of volume and is designated  $V^*$ . Charles and Hillig<sup>(2)</sup> then develop the differential equation for flaw growth in terms of applied stress and flaw geometry. An approximate solution to the differential equation predicts the general shape of the static fatigue curve; i.e., the shape of a plot of  $S/S_N$  vs.  $\tau$  where  $S$  is applied stress under experimental conditions,  $S_N$  is measured strength under comparable conditions in an inert atmosphere and  $\tau$  is the delayed failure time. At low stress levels the curve will flatten out and reach a fatigue limit given by:

$$\left( \frac{S}{S_N} \right)_{\text{lim}} = \frac{1 + \frac{3\omega}{\rho}}{2 \beta \quad 6_u} \quad (3)$$

where,

$$\omega = \frac{\square V_m}{2 RT}$$

and  $\rho$  is the radius of curvature at the tip of the advancing flaw,  $\beta = -V^*/RT$  is related to the activation volume discussed above,  $\sigma_u$  is the ultimate cohesive strength of the material under study,  $\gamma$  is the surface free energy between the base material and its corrosion products,  $V_m$  is the molar volume of the material under study,  $R$  is the gas constant, and  $T$  is absolute temperature. The slope of the central straight line portion of the static fatigue curve is given by

$$\left. \frac{d(S/S_N)}{d \log \tau} \right|_{\text{center}} = \frac{RT}{V^* \sigma_u^2} \quad (4)$$

Values of  $(S/S_N)_{\text{lim}}$  and the derivative in (4) are taken from the experimental static fatigue curve,  $\rho$  can be estimated as  $6\text{\AA}$  and  $\sigma_u$  can be taken as  $10^7$  psi. Equations (3) and (4) can then be used to obtain values of  $V^*$  and  $\gamma$ .

For the static fatigue curve of  $\text{MoSi}_2$  at  $500^\circ\text{C}$  in air shown in Figure 1, we calculate  $V^* = 2.4$  cc and  $\gamma = 1800$  ergs/cm<sup>2</sup>. Since there was considerable uncertainty in the correct value to choose for  $S_N$ , the derived activation volume and surface energy have only order of magnitude validity. Nonetheless the theory seems to provide a useful framework for selecting pertinent experiments that may help to define the mechanism of peening more clearly.

Charles has applied the ideas outlined above to the steam corrosion of a number of sodium silicate glasses and aluminum oxide, as well as to the atmospheric corrosion of fused silica, quartz, granite, and magnesium oxide (11, 12, 13). For soda-lime glass in steam, Charles was able to verify predicted relationships between delayed failure times and chemical corrosion rates (11).

There seem to be many points of analogy between the corrosion reactions investigated by Charles and the pest reaction in molybdenum disilicide. The corrosion of sodium silicate glasses by water vapor, like the oxidation of  $\text{MoSi}_2$  in the pest range is associated with an induction period of relatively low weight gain, followed by a period of

accelerating rate (11). The induction time for the glasses is dependent upon both temperature and water vapor pressure. With glasses it has been shown that expanded structures corrode more rapidly than compacted ones. Charles therefore postulated that the large triaxial tensile stresses at the tips of flaws would result in a locally expanded structure and hence in an enhanced local rate of oxidation, leading to the increased stress concentration required for delayed failure. With  $\text{MoSi}_2$  porous materials are found to pest much more rapidly than dense ones,<sup>(3)</sup> and a similar mechanism to that in glasses might operate to accelerate the oxidation reaction at a crack tip relative to the periphery. Delayed failure in glass, like pest in  $\text{MoSi}_2$ , has a high temperature cut-off, although the temperature ranges for the two phenomena are quite different. The absence of delayed failure effects at high temperature in glass is ascribed to an increased rate of the overall corrosion process, so that the corrosion rate at crack tips is no longer markedly accelerated relative to the corrosion rate elsewhere. A similar process could operate in  $\text{MoSi}_2$ , since at high temperatures it is the very rapid initial surface oxidation rates which are responsible for the formation of a protective silica film. Alternatively, in  $\text{MoSi}_2$ , it may only be the formation of solid  $\text{MoO}_3$  (c) which is stress dependent. The upper temperature limit of the pest range is approximately the lowest temperature at which molybdenum trioxide vaporizes as rapidly as it forms. The absence of condensed phase  $\text{MoO}_3$  (c) may be responsible for the absence of pest.

## CONCLUSIONS

Single crystals of  $\text{MoSi}_2$  exhibit delayed failure or static fatigue under pesting conditions ( $450\text{--}600^\circ\text{C}$  in an oxidizing atmosphere). Analogous to the attack of glass by water vapor the phenomenon appears to be an environmental effect on the brittle fracture mechanism. The theory of Charles and Hillig which postulates an accelerated growth of surface flaws or cracks due to the corrosion reaction explains the experimental data. Activation volumes, surface energies, etc., calculated from the theory appear to be reasonable.

Whereas single crystals are not subject to pesting in air at  $500^\circ\text{C}$ , pest reaction was induced in single crystals which had been statically loaded in bending. At higher temperatures the corrosion rate at the crack tip is no longer accelerated relative to corrosion rates elsewhere and there is a high temperature cut off. The absence of condensed  $\text{MoO}_3$  may also play a role in the behavior above  $600^\circ\text{C}$ .

Polycrystals of  $\text{MoSi}_2$  pest in the absence of an external stress, and it was postulated that a source of the stress in polycrystals would be thermal in nature; the magnitude of the stress should be determined by the anisotropy of the thermal expansion along different crystallographic axes. Measurements of thermal expansion by high temperature X-ray diffraction failed to show any large anisotropy. However, differential thermal expansion of the order of 10% could exist and not be detected by the method used. Such anisotropy would be sufficient to induce internal stress of the order of 20, --30,000 psi, sufficient to cause failure during pesting. Thermal expansion coefficients should be determined on oriented single crystals using a differential dilatometer.

The wide scatter of measured strength of single crystals of  $\text{MoSi}_2$  under conditions where no pesting takes place makes reliable analysis of the mechanism difficult. More precise base line strength is needed. A large number of samples could be tested using a constant surface treatment; however, this is expensive and time consuming. We believe that more reproducible polycrystals can be prepared by a pack bed technique. Here thin sheets (.010 -- .020") of molybdenum are packed in silicon powder and heat treated at  $\approx 1300^\circ\text{C}$  for several hours in argon. The  $\text{MoSi}_2$  which is formed is dense and free from large cracks or flaws.

#### REFERENCES

1. J. B. Berkowitz-Mattuck, P. E. Blackburn, and E. J. Felten, Trans. A.I.M.E. (Met. Soc.) 233, 1093 (1965).

2. R. J. Charles, J. Appl. Phys. 29, 1549 (1958); *ibid.*, p. 1554.

R. J. Charles, Paper No. (90) in Conference on Fracture, April 12-14, 1959, National Academy of Sciences.

R. J. Charles, Task 9, p. 467 ff, ASD-TR-61-628, Part II, April, 1963.

3. O. Rubisch, Beuchte der Deutschen Keramischen Gesellschaft e.v., 41, 120 (1964).